

# PREPARATION OF ASTAXANTHIN/PYCNOGENOL NANOPARTICLES: A DELIVERY SYSTEM WITH IMPROVED ASTAXANTHIN STABILITY AND BIOAVAILABILITY

CHẾ TẠO HẠT NANO ASTAXANTHIN/PYCNOGENOL: MỘT HỆ THỐNG PHÂN PHỐI CẢI THIỆN ĐỘ ỔN ĐỊNH VÀ KHẢ DỤNG SINH HỌC CHO ASTAXANTHIN

Ho Thi Oanh<sup>1</sup>, Hac Thi Nhung<sup>1,2</sup>, Nguyen Hong Tham<sup>1</sup>, Doan Tien Dat<sup>1,2</sup>, Nguyen Duc Tuyen<sup>1</sup>,  
Nguyen Thi Sang<sup>3</sup>, Nguyen Yen Thanh<sup>3</sup>, Truong Cong Doanh<sup>4</sup>, Hoang Mai Ha<sup>1,2,\*</sup>

DOI: <http://doi.org/10.57001/huiv5804.2024.276>

## ABSTRACT

Astaxanthin (AST) and pycnogenol (PYC) are natural bioactive compounds commonly used in pharmaceuticals and functional foods due to their highly antioxidant activity and potential health benefits. However, the widespread application of astaxanthin is hindered by its poor water solubility and highly unsaturated structure. In this study, nanoparticles co-delivering astaxanthin and pycnogenol (NAP) were fabricated to enhance the dispersibility, stability, and bioavailability of astaxanthin. The particle size, dispersion index, zeta potential ( $\zeta$ ), and morphology of the nanoparticles were characterized, revealing that the NAP were spherical, had a negative surface charge, and an average particle size in the range of 70 - 91nm with a narrow size distribution. X-ray diffraction (XRD) demonstrated that AST existed in an amorphous form within the NAP. Notably, the excellent water dispersibility and high stability of the astaxanthin/pycnogenol nanoparticles significantly enhanced cellular uptake, with absorption efficiency being 12 times higher than that of pure astaxanthin. Furthermore, the antioxidant activity was notably improved. These findings suggest that the astaxanthin/pycnogenol nanoparticles is an ideal formulation of astaxanthin, offering potential for the development of new functional foods.

**Keywords:** Astaxanthin, pycnogenol, nanoparticles, cell uptake, antioxidant activity.

## TÓM TẮT

Astaxanthin (AST) và pycnogenol (PYC) là các hợp chất có hoạt tính sinh học tự nhiên thường được sử dụng trong dược phẩm và thực phẩm chức năng bởi hoạt tính chống oxy hóa cao và lợi ích tiềm năng của chúng đối với sức khỏe. Tuy nhiên, việc ứng dụng rộng rãi astaxanthin bị hạn chế do khả năng hòa tan trong nước kém và cấu trúc không bão hòa cao. Trong nghiên cứu này, các hạt nano đồng phân phối astaxanthin và pycnogenol (NAP) đã được chế tạo để nâng cao khả năng phân tán, tính ổn định và sinh khả dụng cho astaxanthin. Kích thước hạt, chỉ số phân tán, thế zeta ( $\zeta$ ) và hình thái của các hạt nano đã được xác định, cho thấy rằng các hạt nano NAP có dạng hình cầu, có điện tích bề mặt âm và kích thước hạt trung bình trong khoảng từ 70 - 91nm với dải phân bố kích thước hẹp. Giải đồ nhiễu xạ tia X đã chứng minh rằng AST tồn tại ở dạng vô định hình trong các hạt nano NAP. Đặc biệt, khả năng phân tán tốt và tính ổn định cao trong nước của các hạt nano astaxanthin/pycnogenol đã tăng cường khả năng hấp thu vào trong tế bào một cách đáng kể, với hiệu quả hấp thu gấp 12 lần so với astaxanthin tự do. Ngoài ra, hoạt tính chống oxy hóa cũng được cải thiện đáng kể. Những kết quả này cho thấy rằng hệ nano astaxanthin/pycnogenol là một công thức bào chế lý tưởng của astaxanthin, mở ra tiềm năng phát triển các loại thực phẩm chức năng mới.

**Từ khóa:** Astaxanthin, pycnogenol, hạt nano, hấp thu tế bào, khả năng chống oxy hoá.

<sup>1</sup>Institute of Chemistry, Vietnam Academy of Science and Technology, Vietnam

<sup>2</sup>Graduate University of Science and Technology, Vietnam Academy of Science and Technology, Vietnam

<sup>3</sup>Faculty of Engineering Physics and Nanotechnology, VNU University of Engineering and Technology, Vietnam

<sup>4</sup>Hanoi University of Industry, Vietnam

\*Email: [hoangmaiha@ich.vast.vn](mailto:hoangmaiha@ich.vast.vn)

Received: 10/6/2024

Revised: 23/8/2024

Accepted: 27/8/2024

## 1. INTRODUCTION

Nowadays, natural compounds like astaxanthin and pycnogenol are receiving significant attention for their roles in functional foods and nutraceuticals aimed at improving human health, well-being, and performance [1, 2]. Astaxanthin, a red pigment belonging to the carotenoid group, is found in red yeast, the microalga *Haematococcus pluvialis*, and aquatic organisms such as salmon, shrimp, crab, and lobster [3]. Astaxanthin has various advantageous biological activities, including strong antioxidant capacity, anti-inflammatory effects, inhibition of cancer cell proliferation, prevention of atherosclerosis, and reduction of symptoms related to cardiovascular, respiratory, and nervous system diseases [4-6].

Astaxanthin has a molecular formula of  $C_{40}H_{52}O_4$ , with a structure comprising 11 conjugated double bonds, 2  $\beta$ -ionone rings, and hydroxyl groups (Fig. 1) [7]. The conjugated double bond system is responsible for astaxanthin's red color and its strong antioxidant activity. However, this molecular structure with many conjugated double bonds makes astaxanthin unstable and easily degraded by oxidative agents, light, and temperature [8]. Moreover, astaxanthin is a hydrophobic molecule with low oral bioavailability, which also limits its application potential [9].

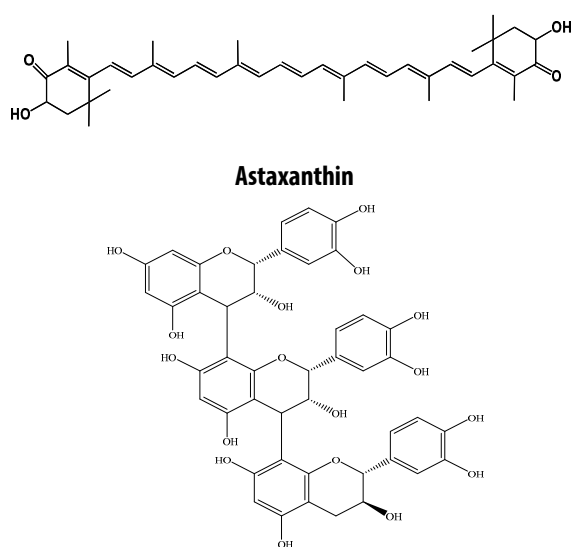


Fig. 1. Molecular structures of astaxanthin and pycnogenol

Pycnogenol is a flavonoid extracted from the bark of the French maritime pine, carrying many beneficial pharmacological properties [10]. It is well-known for its excellent antioxidant and anti-inflammatory capabilities, which help enhance cardiovascular health, improve

blood circulation, protect neural cells, manage pain, and eliminate free radicals [11]. The main component of pycnogenol is procyanidin (Fig. 1), accounting for 70 - 85%, which are biological polymers of catechin and epicatechin subunits, recognized as important components in human nutrition [12].

Several reports have demonstrated that the combination of natural bioactive compounds in composite products yields synergistic effects, enhancing stability and bioactivity compared to using individual compounds alone [13-15]. Flavonoid compounds such as pycnogenol, quercetin, and kaempferol can create synergistic effects, enhancing the stability of compounds with many conjugated double bonds, such as astaxanthin, lycopene, and beta-carotene. However, research on the fabrication of nanoparticle systems containing both carotenoid and flavonoid compounds remains limited, particularly in successfully preparing nanoparticles co-delivering astaxanthin and pycnogenol.

Therefore, the application of nanotechnology to prepare astaxanthin/pycnogenol nanoparticles to improve the dispersibility, stability, absorption efficiency, and antioxidant activity of astaxanthin is a novel and necessary scientific direction. In this study, astaxanthin/pycnogenol nanoparticles were prepared using two surfactants, tween 80 and lecithin, with beta-cyclodextrin as the encapsulating agent, followed by freeze-drying to obtain the nanopowder. The total content of the natural compounds astaxanthin and pycnogenol in the nanoparticle system reached up to 10%. Subsequently, the nanoparticles were analyzed for their structure, morphology, and stability, while also evaluating biological activities such as cellular uptake capability and antioxidant potential.

## 2. MATERIALS AND METHODS

### 2.1. Material

Astaxanthin is a compound extracted from algal biomass *Haematococcus pluvialis*, with a purity of over 96% [16].

Pycnogenol (containing 70 - 85% procyanidins) is a commercial product extracted from the bark of the French maritime pine.

Surfactants: tween 80 and lecithin from Sigma-Aldrich, USA.

Encapsulating agent: beta-cyclodextrin purchased from AKScientific, USA.

All solvents used in this study were of analytical or HPLC grade.

## 2.2. Preparation of nanoparticles co-delivering astaxanthin and pycnogenol (NAP)

Astaxanthin and pycnogenol were mixed at different ratios (Table 1). These active ingredients were then dissolved in tetrahydrofuran solvent using a magnetic stirrer (RCT basic IKAMAG® safety control, Germany) at 550rpm for 30 minutes. Subsequently, tween 80 and lecithin, the two surfactants, were simultaneously added, and the stirring speed was increased to 650rpm. After stirring for 30 minutes, the organic phase was slowly dripped into the aqueous phase containing the carrier beta-cyclodextrin. The resulting solution is further homogenized under an Ultra-Turrax (T18 IKA, Germany) for 45 minutes to obtain a uniform nanoparticle system. The LABCONCO freeze-dryer was then used to obtain astaxanthin/pycnogenol nanopowder. Freeze drying was performed with a collector temperature of -50°C and a vacuum of 0.050mBar. The schematic fabrication procedure for the astaxanthin/pycnogenol nanopowder is presented in Fig. 2.

Table 1. Composition for each of the prepared nanoparticle formulations

Formulation	AST (mg)	PYC (mg)	T80 (mg)	Lec (mg)	β- CD (mg)	Loading Bioactive Compound (%)	
						AST	PYC
NAP1	10	30	80	40	240	2.5	7.5
NAP2	20	20	80	40	240	5.0	5.0
NAP3	30	10	80	40	240	7.5	2.5

**Abbreviations:** T80 (Tween 80), Lec (Lecithin), and β-CD (β-cyclodextrin).

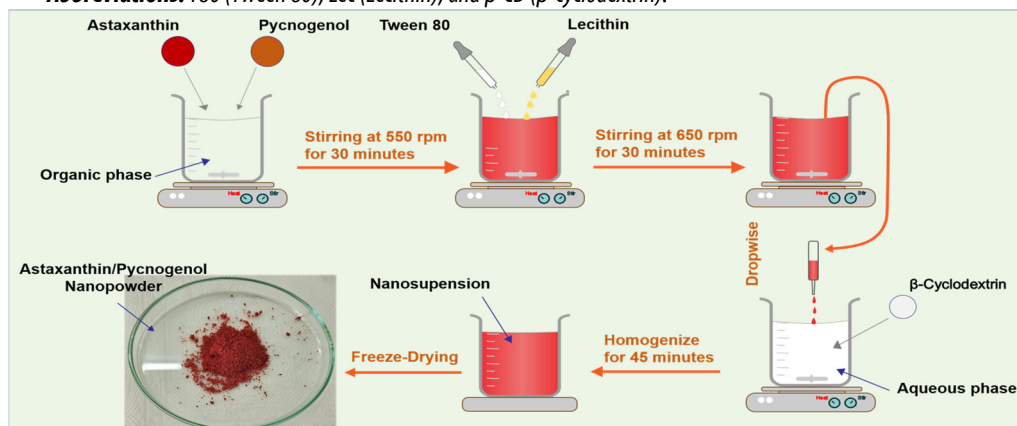


Fig. 2. Schematic illustration of astaxanthin/pycnogenol nanopowder formation

## 2.3. Characterization of nanoparticles co-delivering astaxanthin and pycnogenol

### 2.3.1. Fourier transform infrared spectroscopy (FTIR)

The FT-IR spectra of astaxanthin, pycnogenol and astaxanthin/pycnogenol nanoparticle systems were measured using a PerkinElmer GX instrument (USA) over the range of 400 - 4000cm<sup>-1</sup>.

### 2.3.2. X-ray Diffraction

The crystalline states of astaxanthin, pycnogenol, and the astaxanthin/pycnogenol nanoparticle systems were assessed by a D8-ADVANCE diffractometer (Bruker, Germany) with a 2θ angle range from 10 to 70°, utilizing a CuK<sub>α</sub> radiation source operated at 30mA and 40kV.

### 2.3.3. Particle size, polydispersity index (PDI), and zeta potential

The mean particle diameter, polydispersity index and surface potential (ζ-potential) of the astaxanthin/pycnogenol nanoparticles in the dispersions were measured by dynamic light scattering (DLS) using a Litesizer™ 500 instrument (Anton Paar, Austria). All measurements were conducted at 25°C and each sample was analyzed in triplicate.

### 2.3.4. Morphology

Transmission electron microscopy (TEM) was used to determine the shape and surface morphology of the produced nanoparticles. The morphological investigation of nanoparticles co-delivering astaxanthin and pycnogenol was carried out according to the method described by Fuguo Liu et al. (2018). The samples were observed directly without any staining.

## 2.4. Cell viability assay

The toxicity of the astaxanthin/pycnogenol nanosystems at different concentrations on HepG2 cells was evaluated using the MTT ((3-[4,5-dimethylthiazol-2-yl]-2,5-diphenyl tetrazolium bromide) assay. HepG2 cells were seeded into 96-well plates at a density of 0.5 × 10<sup>5</sup> cells per well and incubated overnight at 37°C with 5% CO<sub>2</sub>. After incubation, the old medium was replaced with fresh medium containing different concentrations (20 and

100µg/mL) of astaxanthin (AST), pycnogenol (PYC), and the nanosystem co-delivering astaxanthin and pycnogenol (NAP2). Untreated cells in wells were used as controls. HepG2 cells were incubated with AST, PYC, and NAP2 for 2 hours. Subsequently, 5mg/mL MTT reagent was added to the samples, and the cells were incubated for an additional 3 hours until purple formazan products developed. Formazan crystals formed in the cells were dissolved by adding 100µL of DMSO, followed by further incubation for 2 hours. The absorbance was measured using a Multiskan SkyHigh microplate spectrophotometer (Thermo Scientific) at a wavelength of 570nm. Cell viability was calculated using the following expression:

$$\text{Cell Viability} = (\text{OD}_{570\text{nm sample}} / \text{OD}_{570\text{nm control}}) * 100\%$$

### 2.5. Antioxidant activity studies

1,1-Diphenyl-2-picrylhydrazyl (DPPH) is a free radical generator used to screen the antioxidant effects of substances under study. Antioxidant activity is demonstrated by the reduction of DPPH color, determined spectrophotometrically at a wavelength of 517nm. In summary, 100µL of a 0.2mM DPPH solution was prepared in methanol (MeOH), and then 100µL of nanoparticles co-delivering astaxanthin and pycnogenol (at concentrations of 4, 20, and 100µg/mL) was added. The reaction was allowed to proceed for 30 minutes at 37°C, after which the absorbance of DPPH was measured using a microplate reader (Thermo Fisher Scientific, USA). Ascorbic acid was used as a positive control. The % DPPH radical scavenging activity of the test sample was calculated using the following formula:

$$\% \text{ SA} = (\text{OD}_{\text{control}} - \text{OD}_{\text{sample}}) * 100 / \text{OD}_{\text{control}}$$

### 2.6. Cellular uptake

The absorption capability of astaxanthin/pycnogenol nanoparticles was indirectly determined by comparing the absorption capacity of astaxanthin within nanoparticles to pure astaxanthin in HepG2 cells. The method for evaluating the absorption capacity of astaxanthin in cells was carried out according to the procedure described by Hien et al. [17]. Specifically, HepG2 cells were cultured for 24 hours at a density of  $1 \times 10^6$  cells per dish and then treated with 5µg/mL of free astaxanthin or 100µg/mL of nano astaxanthin/pycnogenol (containing an equivalent amount of 5µg/mL astaxanthin) for 4 hours. After the incubation period, the cells were washed three times with phosphate-buffered saline (PBS), lysed, and centrifuged at 2000rpm for 3 minutes. The concentration of astaxanthin in the cells was determined by high-

performance liquid chromatography (HPLC), as previously reported by Hien et al. [17].

## 3. RESULTS AND DISCUSSION

### 3.1. FTIR and XRD analysis of astaxanthin/pycnogenol nanoparticles

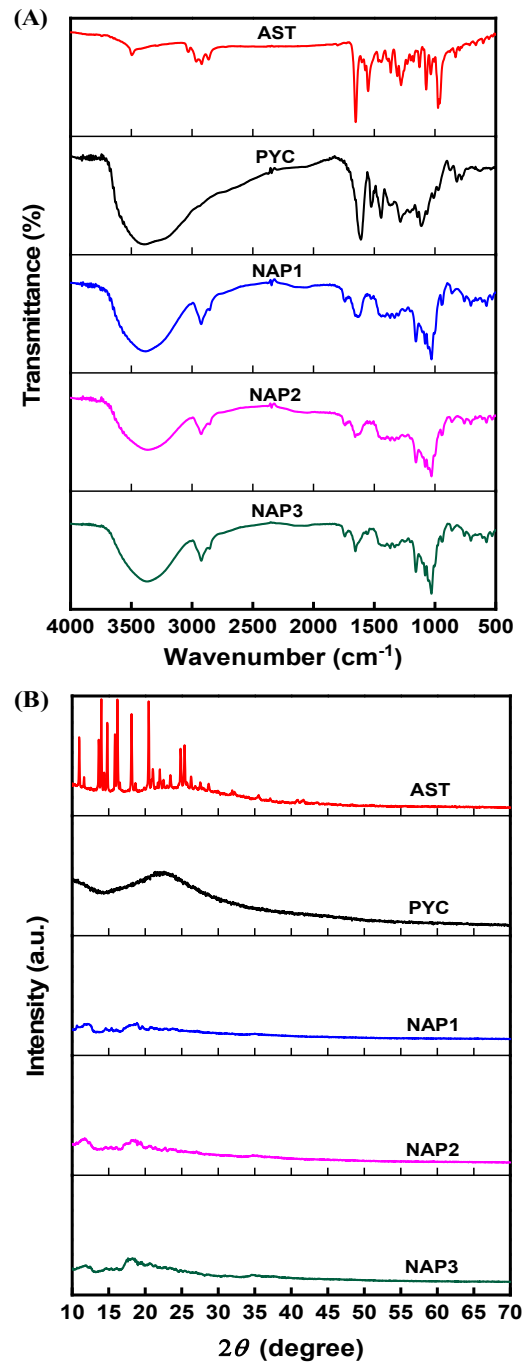


Fig. 3. The FT-IR spectrum (A) and XRD patterns (B) of astaxanthin (AST), pycnogenol (PYC), and astaxanthin/pycnogenol nanoparticles (NAP1, NAP2, and NAP3)

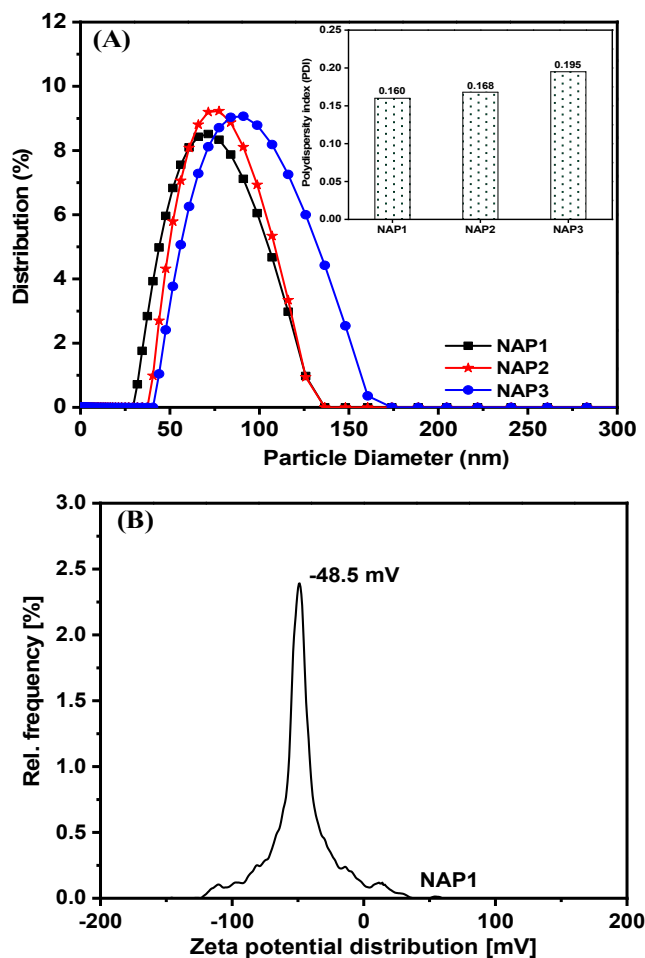
The nano systems were prepared with astaxanthin/pycnogenol ratios of 1/3, 1/1, and 3/1, respectively. Specifically, we examined samples NAP1 (2.5

wt% AST and 7.5 wt% PYC), NAP2 (5 wt% AST and 5 wt% PYC), and NAP3 (7.5 wt% AST and 2.5 wt% PYC). The FTIR spectra of pure astaxanthin, pure pycnogenol, and the nanosystems encapsulating astaxanthin and pycnogenol are shown in Fig. 3A. The strong absorption band of pure astaxanthin at  $1651\text{cm}^{-1}$  is assigned to the C=O stretching vibration peak. Additionally, bands at  $1549\text{cm}^{-1}$  and  $975\text{cm}^{-1}$  correspond to the C=C stretching vibration in aromatic rings and the C-H in the C and C conjugate system, respectively. The characteristic absorption peak at  $2920\text{cm}^{-1}$  indicates the stretching vibration of  $-\text{CH}_3$ . Similar results were also reported in previous studies [18]. The characteristic peak of pycnogenol observed in the broad range of wavenumbers from  $3600$  to  $3015\text{cm}^{-1}$  is assigned to the  $-\text{OH}$  stretching. Additionally, the peak at  $1612\text{cm}^{-1}$  is characteristic of the C=C stretching vibration in aromatic rings. The FTIR spectrum of pycnogenol obtained is completely consistent with previously published studies [19]. All characteristic functional groups of astaxanthin and pycnogenol are present in the FTIR spectra of nanoparticles co-delivering astaxanthin and pycnogenol (NAP1, NAP2, and NAP3). The results indicated that the two active compounds, astaxanthin and pycnogenol, have been successfully physically encapsulated in the nanoparticles.

The XRD pattern was performed on astaxanthin, pycnogenol, and nanoastaxanthin/pycnogenol to obtain information about their crystalline states (Figure 3B). The XRD pattern of astaxanthin shows multiple characteristic peaks with high intensity at  $11.03^\circ$ ;  $13.6^\circ$ ;  $14.9^\circ$ ;  $16.3^\circ$ ;  $18.1^\circ$ ;  $20.6^\circ$ ;  $23.4^\circ$ ;  $24.8^\circ$ ;  $25.6^\circ$  and  $27.5^\circ$ , confirming that pure astaxanthin is in crystalline form, consistent with previous reports [20]. In contrast, the X-ray diffraction pattern of pycnogenol does not exhibit clear diffraction peaks. This can be explained by the chemical composition of pycnogenol, which includes a mixture of phenolic compounds: flavonoids (procyanidins account for 70 - 85%), monomers (catechin, epicatechin, taxifolin), phenolic or cinnamic acids, and their glycosides. For the NAP1, NAP2, and NAP3 nanoparticles, the sharp peaks of astaxanthin also disappeared in the XRD pattern of these systems. This phenomenon indicated that astaxanthin has been loaded into the nanoparticles and has transitioned from a crystalline state to an amorphous form. Changing the crystalline nature through nano formulation is often an ideal way to enhance the solubility of astaxanthin, thereby improving the practical applications of the active ingredient.

### 3.2. Morphology and particle size analysis of nanoparticles co-delivering astaxanthin and pycnogenol

In this study, the morphology, particle size distribution, polydispersity index (PDI), and zeta potential of the nanoparticles co-delivering astaxanthin and pycnogenol were also investigated. The particle size distribution and polydispersity index of the astaxanthin/pycnogenol nanoparticles (Fig. 4A) showed that the average particle diameters for NAP1, NAP2, and NAP3 samples were 70, 78, and 91nm, respectively, with PDI values of 0.164, 0.168, and 0.195. The co-encapsulated astaxanthin and pycnogenol nano systems exhibited a narrow distribution with average particle sizes below 100nm. The zeta potential of the astaxanthin/pycnogenol nanoparticles is presented in Figures 4B-D. The NAP1, NAP2, and NAP3 nanoparticles had a negative charge with relatively high absolute zeta potential values of 48.5, 44.9, and 42.9mV, respectively. According to previous studies, nanoparticles with absolute zeta potential values above 20mV were considered to have high physical stability [21].



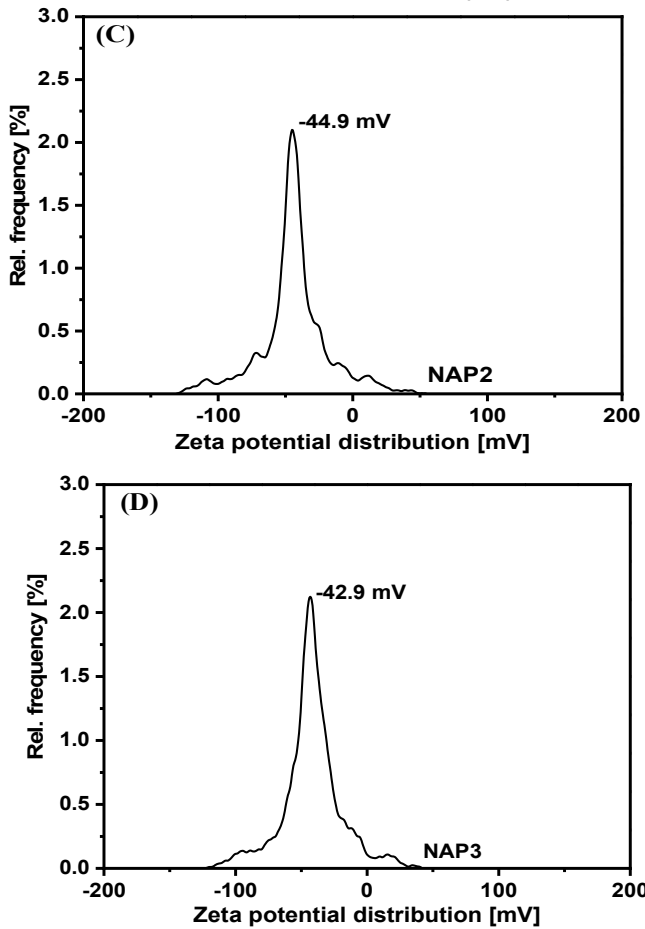


Fig. 4. The size distribution, polydispersity index (A) and zeta potential (B-D) of astaxanthin/pycnogenol nanoparticles

The morphology of astaxanthin/pycnogenol nanoparticles was assessed using transmission electron microscopy (TEM). As depicted in Fig. 5, the nanoparticles exhibited a spherical shape, with variations in particle distribution observed among the NAP1, NAP2, and NAP3 samples. TEM images (Figs. 5A & B) showed that NAP1 and NAP2 nanoparticles were small and spherical with a uniform distribution, whereas NAP3 nanoparticles (Fig. 5C) appeared larger and tended to aggregate. Notably, among the three samples, NAP2 nanoparticles exhibited the most uniform shape and distribution.

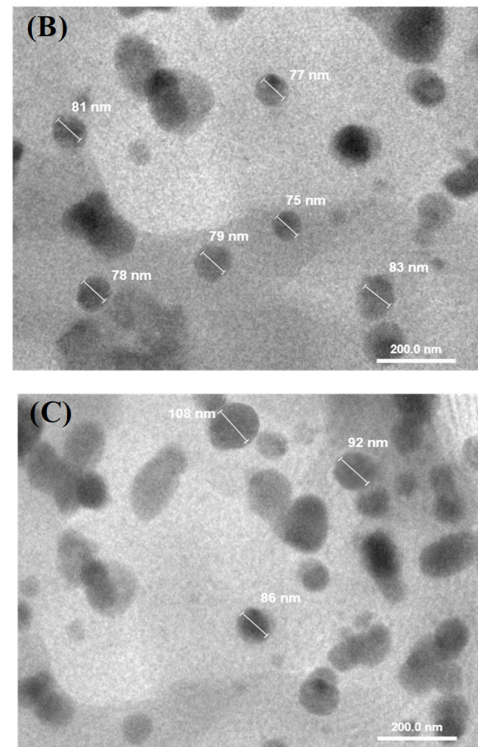
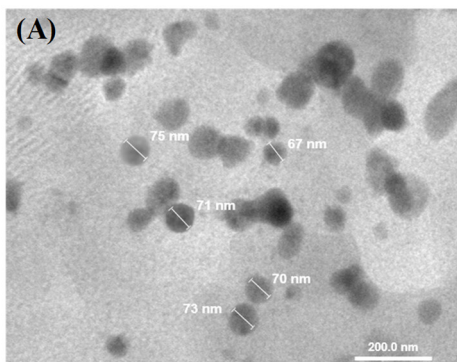
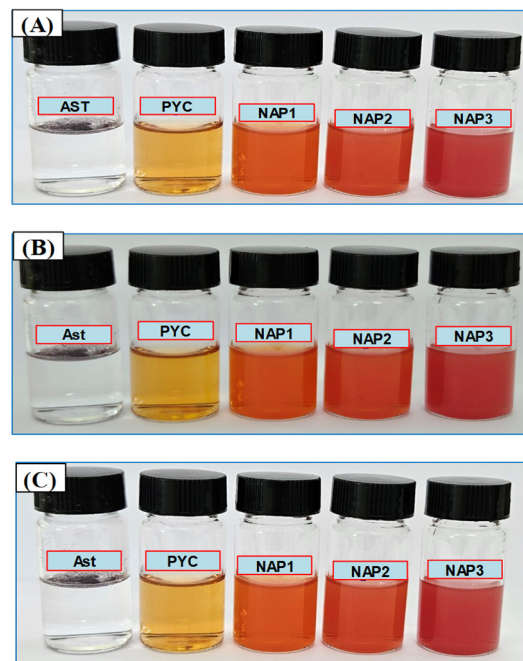


Fig. 5. Transmission electron microscopy (TEM) image of NAP1 (A), NAP2 (B), and NAP3 (C) samples (scale bar = 200nm)

### 3.3. Stability of the nanoparticles co-delivering astaxanthin and pycnogenol

The stability of astaxanthin, pycnogenol, and astaxanthin/pycnogenol nanoparticles was evaluated based on changes in color, particle size, and zeta potential over a 30-day storage period at room temperature (Figs. 6 and 7).



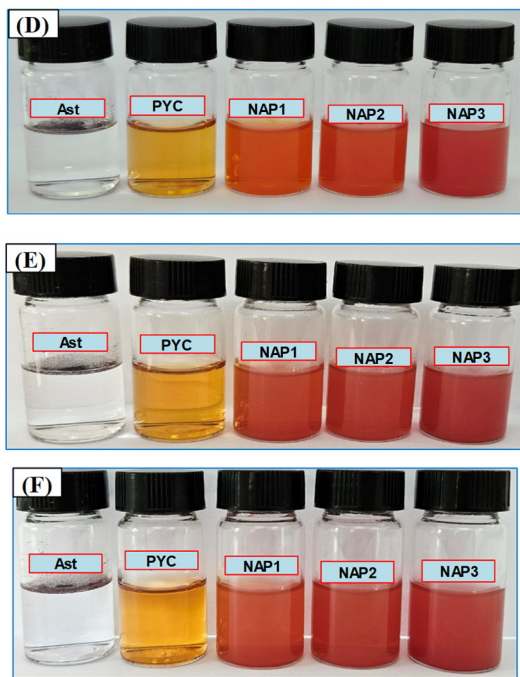


Fig. 6. Photographs of astaxanthin (AST), pycnogenol (PYC), and nanoastaxanthin/pycnogenol (NAP1, NAP2, and NAP3) after storage for different time: starting time (A), 1 day (B), 2 days (C), 7 days (D), 14 days (E), and 30 days (F)

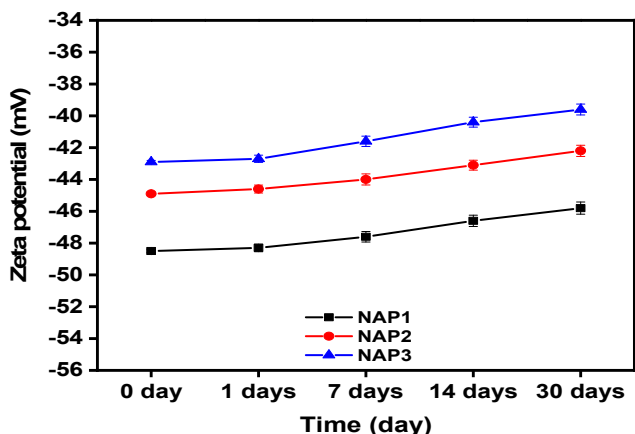


Fig. 7. The variation of zeta potential over time of astaxanthin/pycnogenol nanoparticles in an aqueous environment

Fig. 6 showed that pure astaxanthin was insoluble in water and formed a purple suspension floating on the water surface. In contrast, the nanoparticles co-delivering astaxanthin and pycnogenol exhibited excellent water dispersion, forming a red solution when dispersed in water, with the intensity of the red color increasing in the NAP2 and NAP3 samples. This color change in the solutions was attributed to the increasing astaxanthin content in the nanopowders. After 7 days of storage at room temperature, astaxanthin remained insoluble, while pycnogenol showed signs of sedimentation. The NAP1, NAP2, and NAP3 samples maintained a red color

with no significant changes throughout the storage period. After 30 days, the solutions of the NAP1 and NAP2 samples remained clear, with only the NAP3 showing slightly sedimentation. The Fig. 7 indicated that the zeta potential of astaxanthin/pycnogenol nanoparticles varied slightly after one month. Specifically, the zeta potential of the NAP1, NAP2, and NAP3 samples increased by 5.6% (from -48.5 to -45.8mV), 6.1% (from -44.9 to -42.2mV), and 7.5% (from -42.9 to -39.7mV), respectively. Despite the slight increase in zeta potential values, the nanoparticles remain within the stable range. Therefore, the astaxanthin/pycnogenol nanoparticle systems in this study maintained high stability in aqueous environments over an extended storage period. Among the three nano systems, NAP2 (containing 5% astaxanthin and 5% pycnogenol) exhibited the best physicochemical properties, including a small particle size, uniform distribution, good stability, and high astaxanthin content. Consequently, NAP2 nanoparticles will be selected for evaluating their free radical scavenging ability and cellular uptake.

### 3.4. In vitro cytotoxicity and antioxidant activity of astaxanthin/pycnogenol nanoparticles

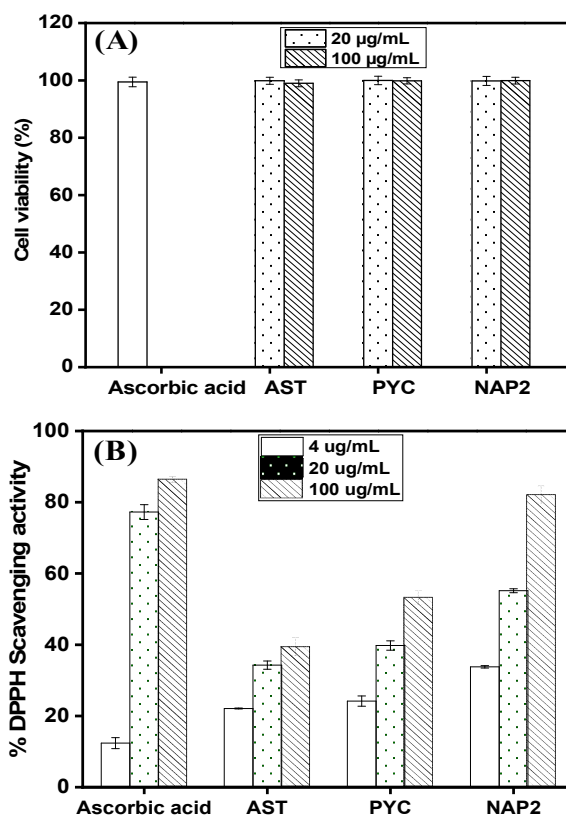


Fig. 8. The MTT assay of HepG2 cells (A) and the analysis of antioxidant activity (B) for astaxanthin, pycnogenol, and astaxanthin/pycnogenol nanoparticles at varying concentrations over 24 hours.

The influence of astaxanthin (AST), pycnogenol (PYC), and nanoastaxanthin/pycnogenol (NAP2) on the viability of HepG2 cells was evaluated through MTT assays. As depicted in Fig. 8A, administration of AST, PYC, or NAP2, even at high concentrations (100µg/mL), did not trigger cell death in HepG2 cells. The percentage of viable cells remained above 99% throughout the experimental period.

Fig. 8B illustrated the antioxidant effects of the astaxanthin/pycnogenol nanoparticles. When comparing NAP2 with free AST or PYC, a significant increase in antioxidant activity of NAP2 was observed. Additionally, according to the study by Hien et al. [16], at a concentration of 100µg/mL, the percentages DPPH scavenging activity of nanoastaxanthin was 43.3%, whereas the activity of astaxanthin/pycnogenol nanoparticles (Fig. 8B) was 82.1%. These results indicated that combining individual agents such as astaxanthin and pycnogenol into a nanoparticle created a synergistic product, enhancing antioxidant activity. The antioxidant effect of NAP2 was evaluated to be equivalent to the ascorbic acid.

### 3.5. Astaxanthin/pycnogenol nanoparticles improve uptake in HepG2 cells

Although astaxanthin possesses many beneficial biological activities, its poor water solubility and low absorption have hindered its practical applications. To address this issue, we successfully developed astaxanthin-encapsulated nanoparticles and evaluated the effects of these nanoparticles on enhancing absorption in HepG2 cells (Fig. 9).

absorption efficiency. Therefore, the use of astaxanthin/pycnogenol nanoparticles markedly enhanced its absorption in HepG2 cells.

### 4. CONCLUSION

This study successfully fabricated nanoparticles co-delivering astaxanthin and pycnogenol, resulting in significant improvements in the dispersion, stability, and bioavailability of astaxanthin. The prepared astaxanthin/pycnogenol nanoparticles had an average particle size below 100nm, with a narrow size distribution and uniform morphology. Notably, the NAP2 nanoparticles containing 5% AST and 5% PYC demonstrated high antioxidant activity and superior cellular uptake efficiency. These findings indicate that astaxanthin/pycnogenol nanoparticles not only represent an advanced and efficient delivery system but also hold significant promise for the development of new functional foods and nutritional products.

### ACKNOWLEDGMENTS

This research is funded by Vietnam Academy of Science and Technology under grant number "UDPTCN 01/22-24".

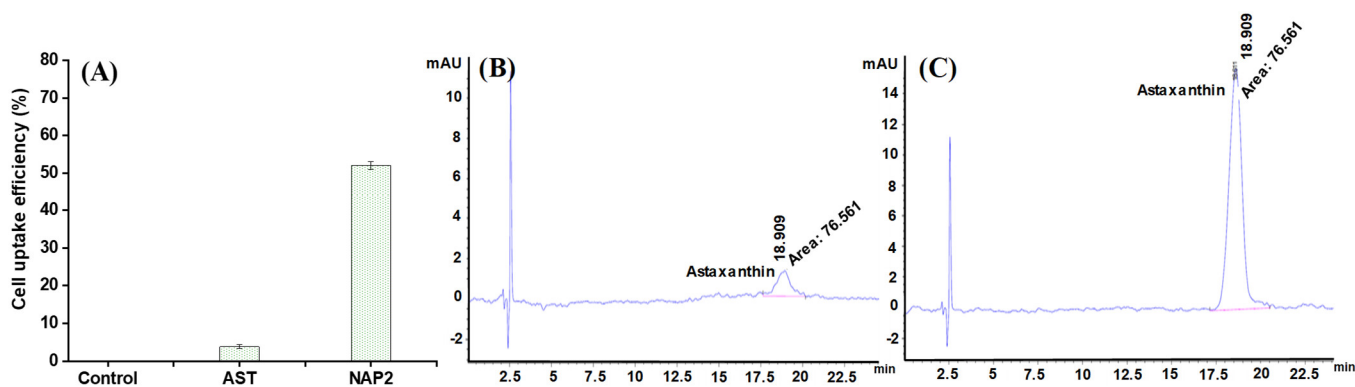


Fig. 9. (A) Cellular uptake and chromatogram of astaxanthin isolated from HepG2 cells which incubated with (B) astaxanthin and (C) astaxanthin/pycnogenol nanoparticles

As shown in Fig. 9, the nano-encapsulated astaxanthin exhibited significantly higher cellular uptake efficiency compared to free astaxanthin, with a 12-fold increase in

### REFERENCES

[1]. Sorrenti V., Burò I., Consoli V., Vanella L., "Recent Advances in Health Benefits of Bioactive Compounds from Food Wastes and By-Products: Biochemical Aspects," *Int J Mol Sci*, 24/3: 2019, 2023.



- [2]. Awuchi CG., Okpala C., "Natural nutraceuticals, especially functional foods, their major bioactive components, formulation, and health benefits for disease prevention - An overview," *J. Food Bioact.*, 19, 97-123, 2022.
- [3]. Shah M. M., Liang Y., Cheng J. J., Daroch M., "Astaxanthin-Producing Green Microalga *Haematococcus pluvialis*: From Single Cell to High Value Commercial Products," *Front Plant Sci.*, 7, 531, 2016.
- [4]. Sztretye M., Dienes B., Gönczi M., Cziráj T., Csernoch L., Dux L., Szentesi P., Keller-Pintér A., "Astaxanthin: A Potential Mitochondrial-Targeted Antioxidant Treatment in Diseases and with Aging," *Oxid Med Cell Longev.*, 200, 1-28, 2019.
- [5]. Si P., Zhu C., "Biological and neurological activities of astaxanthin (Review)," *Mol Med Rep.*, 26/4, 300, 2022.
- [6]. Yao Q., Ma J., Chen X., Zhao G., Zang J., "A natural strategy for astaxanthin stabilization and color regulation: Interaction with proteins," *Food Chem.*, 402, 134343, 2023.
- [7]. Abdelazim K., Ghit A., Assal D., Dorra N., Noby N., Khattab SN., Feky SE El., Hussein A., "Production and therapeutic use of astaxanthin in the nanotechnology era," *Pharmacol Rep.*, 75/4, 771-790, 2023.
- [8]. Santos-Sánchez N., Hernández-Carlos B., Torres-Ariño A., Salas-Coronado R., "Astaxanthin and its Formulations as Potent Oxidative Stress Inhibitors," *Pharmacogn Rev.*, 14/27, 8-15, 2020.
- [9]. Sun J., Wei Z., Xue C., "Recent research advances in astaxanthin delivery systems: Fabrication technologies, comparisons and applications," *Crit Rev Food Sci Nutr.*, 63/19, 3497-3518, 2023.
- [10]. Rohdewald P., "A review of the French maritime pine bark extract (Pycnogenol), a herbal medication with a diverse clinical pharmacology," *Int J Clin Pharmacol Ther.*, 40/4, 158-168, 2002.
- [11]. Nikpayam O., Rouhani MH., Pourmasoumi M., Roshanravan N., Ghaedi E., Mohammadi H., "The Effect of Pycnogenol Supplementation on Plasma C-Reactive Protein Concentration: a Systematic Review and Meta-Analysis," *Clin Nutr Res.*, 7/2, 117-125, 2018.
- [12]. Cizmarova B., Birkova A., Hubkova B., Bolerazska B., "Pycnogenol - extract from French maritime pine bark (*Pinus pinaster*), as an effective antioxidant against superoxide radical," *Funct. Food Rev.*, 1/8, 14, 2021.
- [13]. Yu T., Dohl J., Park YM., Brown LL., Costello RB., Chen Y., Deuster PA., "Protective effects of dietary curcumin and astaxanthin against heat-induced ROS production and skeletal muscle injury in male and female C57BL/6J mice," *Life Sci.*, 288, 120160, 2022.
- [14]. Mazzantiand G., Giacomo SD., "Curcumin and Resveratrol in the Management of Cognitive Disorders: What Is the Clinical Evidence?," *Molecules.*, 21/9, 1243, 2016.
- [15]. Arora I., Sharma M., Tollefsbol TO., "Combinatorial Epigenetics Impact of Polyphenols and Phytochemicals in Cancer Prevention and Therapy," *Int. J. Mol. Sci.*, 20, 4567, 2019.
- [16]. Hien HM., Oanh HT., Quynh QT., Thu NH., Hanh NV., Hong DD., Hoang MH., "Astaxanthin-loaded nanoparticles enhance its cell uptake, antioxidant and hypolipidemic activities in multiple cell lines," *J. Drug Delivery Sci. Technol.*, 80, 104133, 2023.
- [17]. Oanh HT., Hien HM., Tru NV., Hien TT., Hoang MH., "Fabrication of astaxanthin-loaded nanoparticles and their neuroprotective effects on C6 cell lines," *Vietnam J. Chem.*, 1-9, 2024.
- [18]. Mao X., Sun R., Tian Y., Wang D., Ma Y., Wang Q., Huang J., Xia Q., "Development of a solid self-emulsification delivery system for the oral delivery of astaxanthin," *Eur. J. Lipid Sci. Technol.*, 121, 1800258, 2019.
- [19]. Fu C., Yang D., Peh W., Lai S., Feng X., Yang H., "Structure and Antioxidant Activities of Proanthocyanidins from Elephant Apple (*Dillenia indica* Linn.)," *J Food Sci.*, 80/10, 2191-2199, 2015.
- [20]. Hu F., Liu W., Yan L., Kong F., Wei K., "Optimization and characterization of poly(lactic-co-glycolic acid) nanoparticles loaded with astaxanthin and evaluation of anti-photodamage effect in vitro," *R. Soc. Open Sci.*, 6, 191184, 2019.
- [21]. Li MM., Zahi MR., Yuan QP., Tian FB., Liang H., "Preparation and stability of astaxanthin solid lipid nanoparticles based on stearic acid," *Eur. J. Lipid Sci. Technol.*, 118, 592, 2016.

---

#### THÔNG TIN TÁC GIẢ

**Hồ Thị Oanh<sup>1</sup>, Hắc Thị Nhung<sup>1,2</sup>, Nguyễn Hồng Thắm<sup>1</sup>,  
Đoàn Tiến Đạt<sup>1,2</sup>, Nguyễn Đức Tuyền<sup>1</sup>, Nguyễn Thị Sáng<sup>3</sup>,  
Nguyễn Yến Thanh<sup>3</sup>, Trương Công Doanh<sup>4</sup>, Hoàng Mai Hà<sup>1,2</sup>**

<sup>1</sup>Viện Hóa học, Viện Hàn lâm Khoa học và Công nghệ Việt Nam

<sup>2</sup>Học Viện Khoa học và Công nghệ, Viện Hàn lâm Khoa học và Công nghệ Việt Nam

<sup>3</sup>Khoa Vật lý Kỹ thuật và Công nghệ nano, Trường Đại học Công nghệ, Đại học Quốc gia Hà Nội

<sup>4</sup>Trường Đại học Công nghiệp Hà Nội